Assembling amyloid fibrils from designed structures containing a significant amyloid β-peptide fragment

Lars O. TJERNBERG*, Agneta TJERNBERG†, Niklas BARK‡, Yuan SHI§, Bela P. RUZSICSKA§, Zimei BU‖, Johan THYBERG¶ and David J. E. CALLAWAY§[1]

*NEUROTEC, Karolinska Institutet, S141 86 Stockholm, Sweden, †Department of Structural Chemistry, Biovitrum, S112 87 Stockholm, Sweden, ‡Department of Clinical Neuroscience, CMM L8:01, Karolinska Institutet, S171 76 Stockholm, Sweden, §North Shore/LIJ Research Institute, 350 Community Drive, Manhasset, NY 11030-3849, U.S.A., ‖National Institute of Standards and Technology, 100 Bureau Dr Stop 8562, Gaithersburg, MD 20899-8562, U.S.A., and ¶Department of Cell and Molecular Biology, Medical Nobel Institute, Karolinska Institutet, S171 77 Stockholm, Sweden

The amyloid plaque, consisting of amyloid β-peptide (Aβ) fibrils surrounded by dystrophic neurites, is an invariable feature of Alzheimer's disease. The determination of the molecular structure of Aβ fibrils is a significant goal that may lead to the structure-based design of effective therapeutics for Alzheimer's disease. Technical challenges have thus far rendered this goal impossible. In the present study, we develop an alternative methodology. Rather than determining the structure directly, we design conformationally constrained peptides and demonstrate that only certain 'bricks' can aggregate into fibrils morphologically identical to Aβ fibrils. The designed peptides include variants of a decapeptide fragment of Aβ, previously shown to be one of the smallest peptides that (1) includes a pentapeptide sequence necessary for Aβ–Aβ binding and aggregation and (2) can form fibrils indistinguishable from those formed by full-length Aβ. The secondary structure of these bricks is monitored by CD spectroscopy, and electron microscopy is used to study the morphology of the aggregates formed. We then made various residue deletions and substitutions to determine which structural features are essential for fibril formation. From the constraints, statistical analysis of side-chain pair correlations in β-sheets and experimental data, we deduce a detailed model of the peptide strand alignment in fibrils formed by these bricks. Our results show that the constrained decapeptide dimers rapidly form an intramolecular, antiparallel β-sheet and polymerize into amyloid fibrils at low concentrations. We suggest that the formation of an exposed β-sheet (e.g. an Aβ dimer formed by interaction in the decapeptide region) could be a rate-limiting step in fibril formation. A theoretical framework that explains the results is presented in parallel with the data.

Key words: Alzheimer's disease, β-sheet, electron microscopy, molecular modelling, pair correlation.

INTRODUCTION

The polymerization of the 40–42 residue amyloid β-peptide (Aβ) into protease-resistant, insoluble fibrils is an important step in the pathogenesis of Alzheimer's disease [1,2]. Numerous studies have shown that Aβ, a proteolytic fragment generated from the amyloid precursor protein (APP), becomes neurotoxic on polymerization [3–6]. There are several steps in this process that could be the targets for pharmacological intervention: modulation of the expression of the APP, blocking amyloidogenic processing or promoting non-amyloidogenic processing of APP or inhibiting Aβ-polymerization. The last option is an attractive target since it is a pathway without any known biological role. Thus selective polymerization inhibitors would not affect normal cellular functions.

Therapeutic strategies based on the rational design of aggregation inhibitors require knowledge of the molecular structure of amyloid fibrils. Because of the high tendency of Aβ to aggregate into insoluble fibrils, it has not been possible to obtain this structural information by conventional methods, such as X-ray crystallography or NMR. The NMR studies have been limited to Aβ dissolved in organic solvents or buffers with high concentrations of detergents [7–9]. These studies indicate that the peptide to a large extent adopts an α-helix secondary structure. When Aβ is dissolved in buffers free from organic solvents and detergents, and analysed using CD spectroscopy, unordered structures dominate [10]. High-resolution X-ray studies have not been possible, as Aβ does not form crystals. However, fibre diffraction has been used to study fibrils of Aβ. When the fibrils were aligned in a magnetic field, it was possible to resolve several reflections. The most prominent of these were 4.8 Å (1 Å = 0.1 nm), corresponding to the distance between two peptide strands in a cross β-sheet conformation (the strands are orthogonal to the fibre axis), and 10 Å, corresponding to the intersheet distance of two protofilaments. Also present was a reflection at 9.6 Å, which is the true repeat distance for peptide chains in an antiparallel conformation [11,12]. The cross β-sheet structure of the fibrils could be revealed in mathematically filtered cryo-electron micrographs [12]. IR spectroscopy studies of Aβ support an antiparallel alignment of Aβ in the fibrils [13]. However, solid-state NMR studies suggest that the alignment is parallel [14,15]. Binding studies and substitution studies have shown that residues 16–20 in Aβ (Aβ^{16-20}) are crucial for Aβ fibril formation, and that these residues interact with a similar region in Aβ [16,17]. In line with these observations, refined X-ray diffraction data showed a core of Aβ^{16-20} in the fibrils [18], and compounds binding to this region were found to interfere with fibril formation [16,17]. Taken together, these data suggest that Aβ goes from an unordered or α-helical (depending on solvent) secondary structure in solution to a parallel or antiparallel

Abbreviations used: Aβ, amyloid β-peptide; APP, amyloid precursor protein; EM, electron microscopy; TFE, trifluoroethanol; 26SS, C**HQKLVFFAED**YNGK**HQKLVFFAED**C; 28SS, C**HQKLVFFAED**DYNGK**HQKLVFFAED**SC.

[1] To whom correspondence should be addressed (e-mail callaway@indigo.picower.edu).

β-sheet structure in fibrils. Residues in the region Aβ^{16-20}, from adjacent peptide strands, are in close proximity in the fibrils.

Many fragments from Aβ can form fibrils, e.g. Aβ^{25-35} and Aβ^{14-23} [19,20]. We choose to study the decapeptide Aβ^{14-23} since it contains the region Aβ^{16-20}, which is critical for Aβ fibril formation and mediates the strongest Aβ–Aβ binding. The fibrils generated by the decapeptide are very similar to those formed by full-length Aβ, as shown by electron microscopy (EM) [20], X-ray diffraction, Congo Red binding and birefringence (unpublished work). We applied this information to evolve a detailed structural model [20] of fibrils formed by the decapeptide using substitution studies, cross-strand correlations between residue pairs in β-sheets [21] and molecular modelling. Based on the information above, it is natural to hypothesize that the Aβ^{14-23} decapeptide fibrils have a molecular structure similar to the core of full-length Aβ fibrils. Thus this decapeptide could be used as a model peptide for fibril formation, enabling experiments, which were not possible with full-length Aβ.

In the present study, we initiate a new approach aimed at understanding the nature of Aβ aggregation. It is based on the idea of creating peptide 'bricks' of known secondary structure, and then determining which bricks are capable of self-assembly into fibrils and which are not. These bricks include the decapeptide and variants thereof. The structural motif of the bricks that aggregate is as predicted by the model. In other words, rather than determining the structure of amyloid fibrils directly, we explicitly construct several, and show that the requirements of their design are in accord with theoretical precepts. The theoretical methodology utilizes a statistical analysis of the relative probability that a given residue pair is found adjacent in an antiparallel β-sheet (i.e. the pair correlation). The pair correlation yields an estimate of the relative free energy of interaction between a given residue pair. From this free energy of interaction between all residue pairs in and between bricks, it is possible to predict which bricks can continue to assemble into fibrils. The experimental results confirm the theoretical predictions.

Table 1 The five possible antiparallel alignments of the decapeptide Aβ^{14-23}

There are five possible ways of aligning the decapeptide Aβ^{14-23} in an antiparallel β-sheet dimer, provided that at least nine residues should be involved in van der Waals contacts and at least eight hydrogen bonds should form between the backbones of the two strands. The probability of an alignment is calculated from the side-chain pair correlations within antiparallel β-sheets according to Wouters and Curmi [21]. Hydrogen-bonded residue pairs (two bonds per residue pair) are in boldface with a dot between, and C-termini are marked with '–'.

Number	Alignment	Probability P	G^0 (kcal/mol)	vdW contacts	Hydrogen bonds
1	–D**E**A**F**F**V**L**K**Q**H** H**Q**K**L**V**F**F**A**E**D**–	81	−2.56	9	10
2	–D**E**A**F**F**V**L**K**QH HQ**K**L**V**F**F**A**E**D–	7.8	−1.20	9	8
3	–D**E**A**F**F**V**L**K**Q**H** H**Q**K**L**V**F**F**A**E**D**–	1.4	−0.20	10	10
4	–D**E**A**F**F**V**L**K**Q**H** **H**Q**K**L**V**F**F**A**E**D–	0.19	+0.97	9	10
5	–D**E**A**F**F**V**L**K**Q**H** **H**Q**K**L**V**F**F**A**E**D**–	0.12	+1.25	9	8

Table 2 Rotated representations of alignments 1–3 of the decapeptide Aβ^{14-23}

The representations of the alignments of the decapeptide Aβ^{14-23} in Table 1 can be rotated around the x-axis, the y-axis, or both the x- and y-axis. The rotated alignments of the three most probable alignments in Table 1 are listed above. Note that $1 = 1^{xy}$, $1^x = 1^y$, $2 = 2^{xy}$ and $2^x = 2^y$. We will use only 1, 1^x, 2, and ^{x} to describe these rotations respectively.

Rotation around x		Rotation around y		Rotation around x and y	
1^x	H**Q**K**L**V**F**F**A**E**D**– –D**E**A**F**F**V**L**K**Q**H**	1^y	H**Q**K**L**V**F**F**A**E**D**– –D**E**A**F**F**V**L**K**Q**H**	1^{xy}	–D**E**A**F**F**V**L**K**Q**H** H**Q**K**L**V**F**F**A**E**D**–
2^x	H**Q**K**L**V**F**F**A**E**D**– –D**E**A**F**F**V**L**K**Q**H**	2^y	H**Q**K**L**V**F**F**A**E**D**– –D**E**A**F**F**V**L**K**Q**H**	2^{xy}	–D**E**A**F**F**V**L**K**Q**H** H**Q**K**L**V**F**F**A**E**D**–
3^x	H**Q**K**L**V**F**F**A**E**D**– –D**E**A**F**F**V**L**K**Q**H**	3^y	H**Q**K**L**V**F**F**A**E**D**– –D**E**A**F**F**V**L**K**Q**H**	3^{xy}	–D**E**A**F**F**V**L**K**Q**H** **H**Q**K**L**V**F**F**A**E**D**–

EXPERIMENTAL

Theoretical framework

Substituted and truncated variants of the Aβ^{14-23} decapeptide do not form fibrils, indicating that all ten residues are involved in fibril formation [20]. Thus it is assumed that there must be at least eight hydrogen bonds (where ten is maximum) per initial dimer, and that at least nine of the ten residues of each decapeptide must overlap. These requirements limit the possible initial antiparallel dimer conformations to five distinct alignments (Table 1). To estimate the relative probability P for each alignment, we used pair correlation data from Wouters and Curmi [21]. This study tabulates the relative probability that a given residue pair was observed in an antiparallel β-sheet conformation in a set of 253 non-redundant protein structures. The probability P_n that a β-sheet alignment n occurs was obtained by multiplying the pair correlations for each adjacent residue pair (e.g. for alignment 1 in Table 1; **DQ** × EK × **AL**, etc.). As the pair correlations are significantly different for residue pairs that are or are not hydrogen-bonded, the pattern of hydrogen bonds must be considered (cf. alignments 1 and 2 in Table 1). The pair-correlation contribution to the free energy of each alignment was calculated according to the Arrhenius formula $\Delta G^0 = -RT \ln P$ at 20 °C ($RT = 0.583$ kcal/mol) and is shown in Table 1. As the free energy of a random peptide is unknown, the free energies obtained by this procedure are *relative* free energies.

Alignments 1 and 4 have the same number of hydrogen bonds and van der Waals contacts, but the probability of alignment 1 is approx. 400 times higher than that for alignment 4. The same comparison can be made between alignments 2 and 5, alignment 2 being approx. 65 times more likely to occur. Therefore, only alignments 1–3 will be considered for further analysis. By rotating the above alignments around the x- and y-axis, it is possible to achieve different spatial arrangements of the alignments. For alignments 1–3, these rotations are listed in Table 2.

The propagation of alignments is restricted to alignments 1–3 (and their rotations) and depends on the hydrogen-bonding pattern of the exposed decapeptide strand. For example, the only alignments that can follow alignment 1 are alignments 2^x or 3^y. This requirement will be written $1 \rightarrow 2^x, 3^y$. The possible propagation of alignments is listed in Table 3.

Table 3 Possible alignment propagations

The alignment of additional decapeptides to the dimers 1–3 are restricted by the hydrogen-binding patterns. All the possible alignment propagations are listed.

$1 \rightarrow 2^x, 3^y$	$1^x \rightarrow 2, 3$		
$2 \rightarrow 1^x, 3^x$	$2^x \rightarrow 1, 3^{xy}$		
$3 \rightarrow 2^x, 3^y$	$3^x \rightarrow 1, 3^{xy}$	$3^y \rightarrow 2, 3$	$3^{xy} \rightarrow 1^x, 3^x$

Table 4 Possible alignment patterns in fibrils

The three most probable models of fibrils formed from the decapeptide Aβ^{14-23}, based on the possible alignments (listed in Tables 1 and 2) and the possible alignment propagations (Table 3). Here, '•' represents hydrogen bond pairs formed within a dimer and '|' represents hydrogen bond pairs formed between dimers. Thus model 1 can be assembled from dimers constrained to adopt alignment 1 and models 2 and 3 can be assembled from dimers constrained to alignment 3.

Model	Alignment	Probability P	G^0 (kcal/mol)	vdW contacts	Hydrogen bonds
1	HQKLVFFAED– }1^x –DEAFFVLKQH }2 HQKLVFFAED– }1^x –DEAFFVLKQH }2 HQKLVFFAED–	4.0×10^5	−7.51	36	36
2	HQKLVFFAED– }3^x –DEAFFVLKQH }1 HQKLVFFAED– }3^y –DEAFFVLKQH }2 HQKLVFFAED–	1.2×10^3	−4.15	38	38
3	HQKLVFFAED– }3^y –DEAFFVLKQH }3 HQKLVFFAED– }3^y –DEAFFVLKQH }3 HQKLVFFAED–	3.8×10^0	−0.78	40	40

If the cost of both lost hydrogen bonds and van der Waals interactions is negligible, the favoured fibril aggregation mode must involve only alignments 1 and 2. The favoured mode then is $1^x \rightarrow 2 \rightarrow 1^x \rightarrow 2 \rightarrow \cdots$ (Table 4, model 1). This pentamer is predicted to be over 10^5 times more likely than a random pentamer, if hydrogen bonds and van der Waals interactions do not contribute. However, if van der Waals interactions are important (as suggested both by Yang and Honig [22] and the observation that all the residues of the decapeptide are essential for fibril formation [20]) and/or hydrogen bonds are significant, the favoured aggregation pattern is $3^y \rightarrow 3 \rightarrow 3^y \rightarrow 3 \rightarrow \cdots$ (Table 4, model 3), although this structure is only approx. four times as probable as a random alignment. Note that if alignment 1 should appear, it leads naturally into the above pattern by the sequence $1 \rightarrow 3^y \rightarrow 3 \rightarrow 3^y \rightarrow \cdots$. Also note that the structure that is predicted to be most stable strongly depends on the values assigned to G^0_{hbond} and G^0_{vdW}, the Gibbs free energies of hydrogen bonds and van der Waals contacts respectively.

Other fibril models are certainly possible. For example, the hexamer repeat $1 \rightarrow 2^x \rightarrow 3^{xy} \rightarrow 1^x \rightarrow 2 \rightarrow 3^x \rightarrow 1 \rightarrow \cdots$ has $G^0 = -7.91$ kcal/mol $+ 56\ G^0_{\mathrm{vdW}} + 56\ G^0_{\mathrm{hbond}}$ (corresponding to $G^0 = -5.27$ kcal/mol $+ 37.3\ G^0_{\mathrm{vdW}} + 37.3\ G^0_{\mathrm{hbond}}$ for a tetramer repeat as described in Table 4), whereas the model $1 \rightarrow 3^y \rightarrow 3 \rightarrow 2^x \rightarrow 1 \rightarrow \cdots$ is degenerate in energy with model 2. It is not necessary to have a periodic pattern, and so the above models could be mixed in fibrils.

This analysis suggests that it should be possible to construct fibrils from dimeric subunits constrained to adopt alignment 1 or 3. Additionally, it should be impossible to make fibrils from substituted dimeric subunits constrained to adopt alignment 1 or 3 that cannot form either of the alignments 2 or 3 between dimers. These predictions are tested experimentally by the procedures below.

Synthesis and purification of peptides

The peptides were purchased from Research Genetics (Huntsville, AL, U.S.A.), and purified on a 150 mm × 7.5 mm PLRP-S column (Polymer Laboratories, Church Stretton, U.K.) using a water/acetonitrile gradient with 0.1 % trifluoroacetic acid. The purified peptides were freeze-dried and stored in a desiccator. The peptides to be cross-linked were allowed to form S–S bonds in Tris-buffered saline. The reaction was followed with Ellman's reagent [5,5′-dithiobis-(2-nitrobenzoic acid)] [23], and was found to be completed after 5 h incubation. After completion of the reaction, the sample was freeze-dried, dissolved in 70 % formic acid and injected on to a Superdex Peptide size-exclusion column (Pharmacia, Uppsala, Sweden). The monomeric fraction was collected and identity was verified with MS.

MS

Identity and purity were verified with electrospray ionization MS using a Quattro triple quadropole (Micromass Limited, Altrincham, Cheshire, U.K.). To evaluate whether the incubated cysteine-containing peptides were in reduced or oxidized forms, matrix-assisted laser desorption ionization–time-of-flight MS was used on a Micromass TofSpec SE (Micromass Limited) in positive-ion reflectron mode. The matrix solution (saturated α-cyano-4-hydroxycinnamate in 50 % acetonitrile) was mixed with the sample in the ratio 1:1 (v/v) before the analysis. Bradykinin and corticotropin (ACTH) residues 18–39 were used as internal standards. The matrix-assisted laser desorption ionization–time-of-flight MS analysis confirmed by the molecular masses that these peptides were oxidized (by an S–S bridge between the N- and C-terminal cysteines).

CD spectroscopy

The freeze-dried peptides had low solubility in water and aqueous buffers. Therefore, they were dissolved in trifluoroethanol (TFE) to a concentration of 200 μM. This solution was diluted with 10 mM phosphate buffer (pH 7.4), containing 100 mM NaF to final peptide concentrations of 10, 3 and 1 μM. The samples were transferred to a 5 mm pathlength cuvette immediately after mixing, and spectra were recorded on an Aviv 62 CD photometer from 260 to 190 nm. The slit widths were set to 1.5 nm, data were collected for 4 s at each nm, and four scans were averaged. The secondary structure was calculated with three different software packages: CONTIN, SELCON and NEURAL NETWORKS [24]. To compensate for the different final concentrations of TFE, the phosphate buffer was supplemented with 4.5 % (1 μM peptide) and 3.5 % TFE (3 μM peptide). There were no detectable differences between samples with a final TFE concentration of 0.5 and 5 % (1 μM peptide) or 1.5 and 5 % (3 μM peptide).

EM

The peptides were dissolved as described above and incubated for 1 week. The samples were centrifuged for 20 min at 20000 ***g*** and the supernatants were aspirated. The pellets were sonicated in 100 μl water for 5 s, and 8 μl of the resulting suspensions were placed on grids covered by a carbon-stabilized Formvar film. After 30 s, excess liquid was withdrawn and the grids were negatively stained with 2 % uranyl acetate in water. The stained grids were examined and photographed in a Philips CM120TWIN electron microscope at 80 kV.

Molecular modelling

The Insight/Discover 2.9.7 program suite (Biosym/MSI, San Diego, CA, U.S.A.) was used. The simulations were performed in vacuum with the dielectric constant set to unity. Default settings were used for all other parameters. Steepest-descent and conjugate gradient minimization schemes were used to optimize the models with the backbones in a β-sheet conformation.

RESULTS

The exact alignment of Aβ in fibrils is not known, but data indicate that the Aβ^{16-20} sequence is important for fibril formation and that these residues interact with similar sequences in adjacent strands in the fibrils [16–18]. The peptide Aβ^{14-23} includes the Aβ^{16-20} motif, forms fibrils, and has been used as a model peptide for fibril formation [20]. In the present study, we have designed a set of peptides constrained to adopt structures mimicking dimers of Aβ^{14-23} aligned in a β-sheet conformation. By shifting the two strands vis-à-vis each other, or making substitutions or deletions of residues important for interstrand interactions in fibrils, we show the alignments that are compatible with fibril formation. The secondary structure as a function of time and concentration was followed by CD and the fibril formation was assessed by EM.

Design of a peptide C**HQKLVFFAED**YNGK**HQKLVFFAED**C (26SS) constrained to adopt alignment 3

To demonstrate that the theoretical framework is consistent with amyloid aggregation patterns, we designed peptide structures containing the decapeptide Aβ^{14-23} sequence that were structurally constrained so as to force the appearance of the above antiparallel motif. The first peptide contained two copies of the decapeptide connected by a four-residue sequence YNGK, frequently found in type 1′ β-turns [25]. Cysteine residues were added at the C- and N-termini to yield a 26-residue peptide, 26SS. Our analysis predicts that the 26SS peptide spontaneously adopts the structure of alignment 3, with an intramolecular antiparallel β-sheet and cysteines that can subsequently be linked by a disulphide bond.

26SS constrained to alignment 3 (rotated as 3′ in Table 2)

```
  CHQKLVFFAEDY
               N
               G
—CDEAFFVLKQHK
```

In amyloid fibrils assembled from this structural subunit, alignment 3 or rotations (Tables 1 and 2) must appear at every other alignment. Allowable propagation patterns must include models 2 and 3 (Tables 3 and 4), or mixtures of them. Moreover, residue substitutions that disrupt the further assembly of this subunit according to the alignment patterns should not form fibrils. We used CD spectroscopy to study the secondary structure and EM to observe whether the peptide formed fibrils.

The 26SS peptide forms an intramolecular β-sheet and assembles into fibrils

The freeze-dried 26SS peptide was dissolved in TFE to a concentration of 200 μM and diluted with 10 mM phosphate buffer (pH 7.4), containing 100 mM NaF to final peptide concentrations of 10, 3 and 1 μM. The sample was transferred to a 5 mm pathlength cuvette immediately after mixing and CD spectra were recorded. The secondary structure was determined

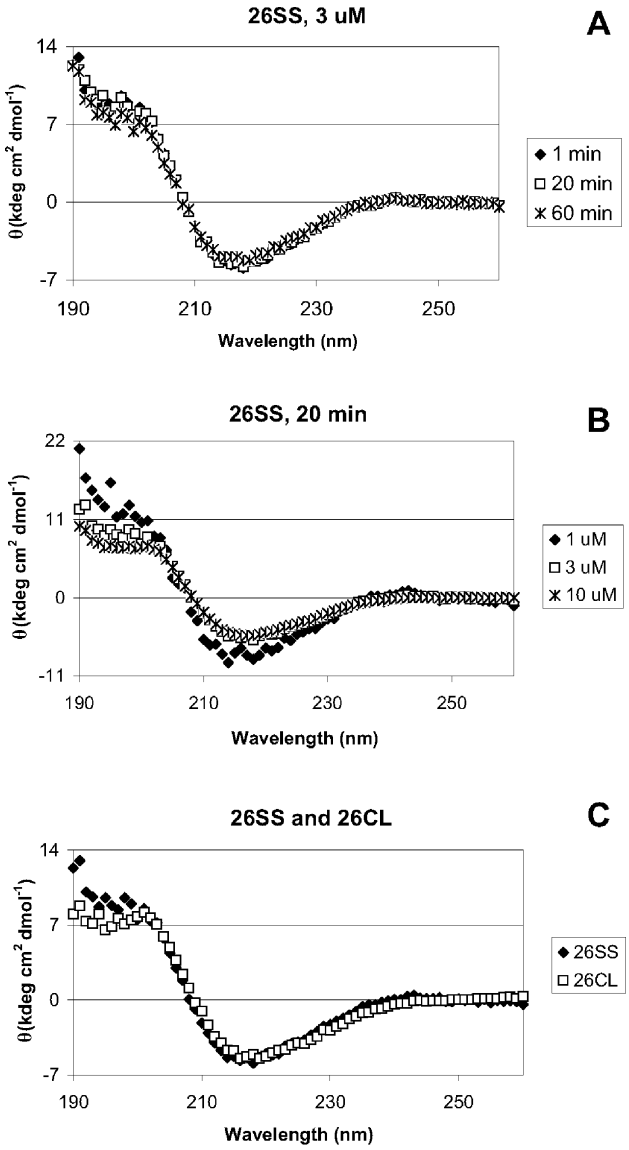

Figure 1 The constrained peptides adopt a β-sheet conformation

CD spectra from 26SS and 26CL. The peptides were dissolved in TFE at 200 μM and diluted in phosphate buffer to the indicated concentrations. The spectra were dominated by a minimum of 217 nm, indicating β-sheet conformation. (**A**) 26SS was diluted to 3 μM and spectra were taken after 1, 20 and 60 min. Note that the β-sheet has formed already at the shortest time-point. (**B**) 26SS was diluted with phosphate buffer at 1, 3 and 10 μM for 20 min. Even at the lowest concentration, the spectrum clearly indicates a β-sheet conformation. (**C**) 26SS and the cross-linked variant 26CL was diluted for 20 min with phosphate buffer at 3 μM. The β-sheet content was in all cases calculated to be approx. 60%. See the Experimental section for details.

by three separate software packages, all yielding 50–60% β-sheet and 15% β-turn. There was no concentration dependence of the results, and no significant differences between spectra taken at 1, 20 and 60 min after dilution of the stock solution (Figures 1A and 1B). This is in sharp contrast with the Aβ^{14-23}, which shows a 'random coil' conformation after 60 min even at 100 μM (results not shown). Since 26SS shows a high amount of β-sheet even at the lowest concentration and at the earliest time point studied, we conclude that the β-sheet is intramolecular. When the samples were examined after 1 week, the CD signal had decreased to less than half of the original value, indicating that the peptide

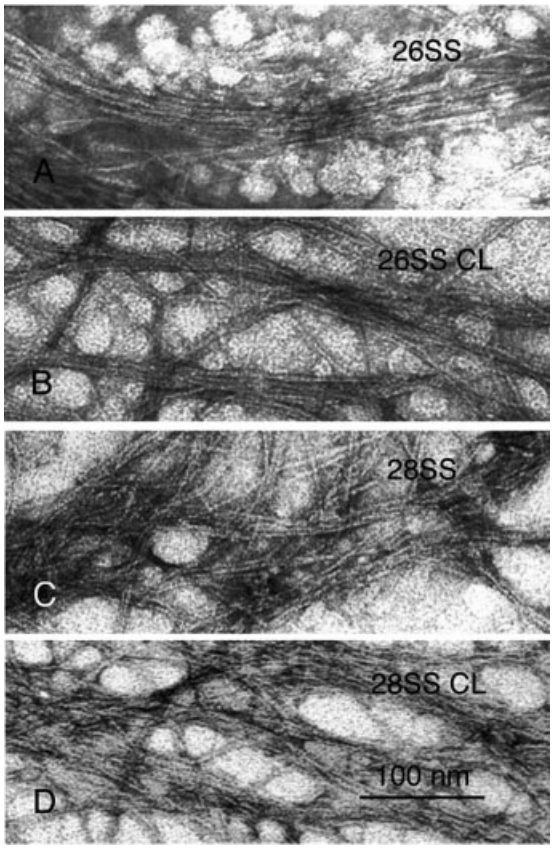

Figure 2 EM on fibrils formed by constrained peptides

The peptides 26SS, 26CL, 28SS and 28CL were incubated for 1 week. The solutions were centrifuged at 20 000 ***g*** and the supernatant was aspirated. Water (100 μl) was added, the pellet was sonicated briefly and 8 μl was placed on grids and negatively stained with uranyl acetate. In all these cases, fibrils similar or identical to those formed by Aβ were observed.

had largely precipitated. EM showed high amounts of fibrils and fibril bundles, morphologically identical to those formed by full-length Aβ or Aβ^{14-23} (Figure 2A).

Preparation and analysis of 26CL, a more constrained variant of 26SS

The above analysis does not rule out the possibility that the 26SS peptide rearranges to form a parallel β-sheet motif during fibrillogenesis, i.e. the intramolecular β-sheet is lost and the peptide forms intermolecular β-sheets in an extended form. Thus the 26SS peptide was incubated and allowed to form disulphide bridges between the cysteines. After 5 h in Tris-buffered saline, assay by Ellman's reagent [23] demonstrated the absence of free sulphydryls, and reversed-phase HPLC analysis confirmed that no reduced peptide was present. The incubate was dissolved in 70 % formic acid and injected on to a Superdex Peptide column and eluted with water/acetonitrile/trifluoroacetic acid (70:30:0.1, by vol.). The monomeric fraction was collected and freeze-dried. The freeze-dried cross-linked monomer, termed 26CL, was then analysed by CD spectroscopy as described above, again yielding a β-sheet content of 50–60 % and a β-turn content of 15–20 % (Figure 1C). Since there was no concentration dependence or significant differences between spectra taken at 1, 20 and 60 min, we again conclude that the β-sheet is intramolecular. Moreover, the alignment is in this case due to the constraint imposed by the S–S bridge, limited to alignment 3. The 10 μM sample was examined with EM after 1 week of incubation. Amyloid fibrils and fibril bundles morphologically indistinguishable from those produced by the reduced peptide were observed (Figure 2B), showing that the fibrils can be formed from a conformationally restricted β-sheet structure as in alignment 3.

Design of a peptide C**HQKLVFFAED**DYNGK**HQKLVFFAED**SC (28SS) constrained to adopt alignment 1

We repeated the above procedures with a peptide of sequence 28SS. As with the 26SS peptide, the sequence YNGK should produce a type 1′ β-turn stabilized by a hydrogen bond between the tyrosine and lysine residues [25]. Thus the structure that is forced to occur will present the decapeptide residues in the conformation of alignment 1^x.

28SS constrained to alignment 1 (rotated as 1^x in Table 2)

CH**Q**K**L**V**F**F**A**E**D**D**Y**
N
G
—**C**S**D**E**A**F**F**V**L**K**Q**H**K**

There is, however, an interesting difference between this peptide and 26SS. The latter (constrained to adopt alignment 3^y) could bind to other 26SS peptides according to alignment 2 or 3. The requirement of a type 1′ β-turn with a hydrogen bond between the tyrosine and lysine residues implies that both Asp-Gln pairs in 28SS are hydrogen-bonded. The 28SS peptide cannot provide the hydrogen bond pattern needed to produce alignment 3 with another 28SS peptide (specifically note the existence of a Gln-Glu hydrogen bond in alignment 3), and alignment 2 must occur every other time. Thus absent of an unusual turn motif without a hydrogen bond between the tyrosine and lysine residues, the only fibrils that can form with 28SS are those of model 1. An energy-minimized representation of model 1 is shown in Figure 3.

Both 28SS and the cross-linked variant 28CL adopt a β-sheet conformation and form fibrils

The 28SS peptide and the cross-linked variant 28CL (prepared in the same way as 26CL) were subjected to the same analysis as 26SS peptide, i.e. CD spectroscopy at different concentrations and EM. Both peptides behaved in all aspects as the shorter variants. Thus both the 28SS and the 28CL peptides produced β-sheet spectra at all concentrations, no significant changes in the spectra were observed during the first 60 min, and amyloid fibrils were observed with EM (Figures 2C and 2D). From the above theoretical and experimental results, we conclude that it is possible to construct fibrils from subunits constrained to adopt alignment 1 or 3.

Substituted, truncated or reversed forms of 26SS and 28SS do not form fibrils

It is essential to establish by negative controls that not every peptide constrained by a turn motif and an S–S bridge automatically form fibrils. Therefore, we constructed three different peptides similar to those investigated above.

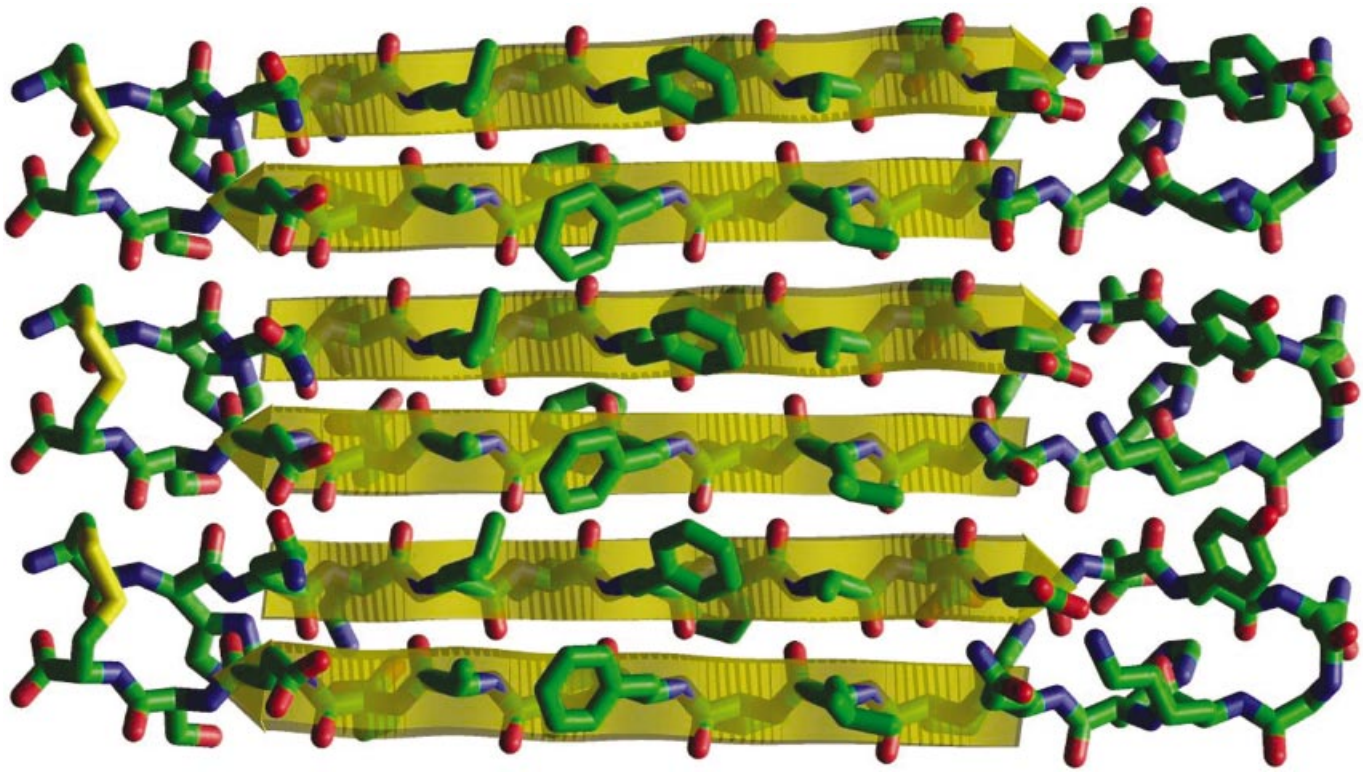

Figure 3 An energy-minimized model of fibrils formed by the 28CL peptide according to fibril model 1

The simulations were performed in vacuum with the dielectric constant set to unity. Default settings were used for all other parameters. Steepest-descent and conjugate gradient minimization schemes were used to optimize the models with the backbones in a β-sheet conformation. The β-sheets were represented by semi-transparent yellow arrows. Color code: green, carbon; red, oxygen; blue, nitrogen; and yellow, sulphur.

28SS$^{Val\text{-}Asp}$ (28SS with Val-Asp substitution)

```
  CHQKLDFFAEDDY
                N
                G
—CSDEAFFDLKQHK
```

The 28SS$^{Val\text{-}Asp}$ peptide, like the 28SS peptide, is forced to adopt the conformation of alignment 1^x. The pair-correlation between Phe and Asp side-chains is zero (with 99.5 % confidence) in a hydrogen-bonded configuration and 1.3 in a non-bonded configuration [21]. The 28SS$^{Val\text{-}Asp}$ peptide should thus form an intramolecular β-sheet, but not produce fibrils since it cannot bind to other 28SS$^{Val\text{-}Asp}$ peptides using alignment 2 or 3. Both fibril models 1 and 2 require alignment 2 to occur at least once every four β-strands, and both models 2 and 3 require alignment 3 to occur. In other words, from Table 1, alignment 1 by itself is insufficient to form fibrils. Thus the theoretical framework outlined here predicts that the 28SS$^{Val\text{-}Asp}$ peptide will not form fibrils (since the necessary alignment 2 cannot form due to the substitutions). Alignments 4 and 5 are still possible, but are predicted to be too weak to form fibrils. The 28SS$^{Val\text{-}Asp}$ peptide was prepared and analysed as described for 26SS and 28SS. CD analysis of 28SS$^{Val\text{-}Asp}$ gave similar spectra, dominated by β-sheet as for 26SS and 28SS. EM observed only small amounts of aggregated material and no fibrils. Hence, the results were in line with the proposed model.

24SS (26SS with Gln deleted)

```
  CHQKLVFFAEDY
              N
              G
—CHQKLVFFAEDK
```

In [20] it was shown that the nonapeptide HKLVFFAED does not form fibrils. Since the 24SS peptide presents precisely this sequence to other 24SS peptides, no fibrils should form unless the introduced turn motif or cysteine residues have a fibrillogenic effect. The 24SS peptide was oxidized, purified, incubated and subjected to EM as described for 26SS. No fibrils were observed, indicating that the turn motif and SS-bridge themselves are insufficient for fibril formation.

26SS^{para} (26SS with parallel-like motif)

```
  CHKLVFFAEDY
            N
            G
—CDEAFFVLKHK
```

This peptide gives similar side-chain interactions as for a parallel, in register alignment (but there are differences due to chirality and backbone interactions). The probability for the above alignment, not including the turn motif and the cysteines is $P = 5.18$.

Assuming that there is a stabilizing hydrogen bond between the tyrosine and lysine residues of the turn, allowed intermolecular alignments include alignments 1^x ($P = 80.96$) and 3^x ($P = 1.40$) from Table 1. The only 'parallel' intermolecular alignment predicted ($P = 5.37$) is bound quite weakly:

HQKLVFFAED-
-HQKLVFFAED

The other possible intermolecular alignment is forbidden because non-bonded histidine pairs are predicted to occur with $P = 0$ (although this result is at 50 % confidence level) [21]:

HQKLDFFAED-
-HQKLVFFAED

The $26SS^{para}$ peptide was subjected to EM analysis according to the same procedure as the other peptides. A few dense aggregates, but no amyloid fibrils could be observed. Thus the turn motif and SS-bridge did not force any of the expected non-fibrillogenic peptides into fibril-competent species. We therefore conclude that the results obtained with the 26SS and 28SS peptides reflect the properties of the $A\beta^{14-23}$ sequence.

DISCUSSION

The polymerization of Aβ into fibrillar deposits in the brain is believed to be a causative step in Alzheimer's disease, and it has been suggested that inhibitors of this process could be of therapeutic use [2]. It has not been possible to determine the structure of Aβ with conventional techniques. In the present study, we employ an alternative approach to obtain a model of the fundamental Aβ–Aβ interactions in fibrils. By using the current knowledge of Aβ structure in combination with a theoretical framework, we construct amyloid building blocks with constrained conformations, and show that these blocks assemble into amyloid fibrils in accordance with the proposed model.

The basic peptide motif $A\beta^{14-23}$ used in this study fulfils several criteria that make it a good model peptide for Aβ fibrils. First, it contains the $A\beta^{16-20}$ sequence. This sequence mediates Aβ–Aβ interactions by binding to the similar region in Aβ, and compounds capable of binding to this region block fibril formation [16,17]. Substitutions in this sequence of Aβ result in peptides incapable of forming fibrils and X-ray diffraction studies indicate that these residues are close to the corresponding residues in neighbouring strands in fibrils [16,18]. Secondly, the decapeptide forms fibrils with the same morphological and tinctorial characteristics as full-length Aβ [20]. Thirdly, C- and N-terminal elongations of the decapeptide do not change fibril morphology or lead to any significant changes in thioflavin T binding [20]. N-terminally truncated Aβ-variants are found both in amyloid plaques and in cerebrospinal fluid, and it is possible that most of the residues N-terminal to $A\beta^{14-23}$ are optional also for fibril formation *in vivo* [26,27]. Residues in the C-terminus of Aβ are important for the kinetics of fibril formation and for the stability of fibrils [28], but there is no evidence that the C-terminal tail should alter the decapeptide interactions in the amyloid fibrils.

In a recent study [20], we proposed the following models of an $A\beta^{14-23}$ dimer (C-terminus labelled with '-'):

HQKLVFFAED-
-DEAFFVLKQH (Dimer 1)

HQKLVFFAED-
-DEAFFVLKQH (Dimer 2)

To investigate whether the suggested interactions between the decapeptides were possible, we synthesized two peptides 26SS and 28SS. These peptides correspond to 2 decapeptides aligned as in 'Dimer 1' (26SS) or in 'Dimer 2' (28SS), connected by a β-turn motif (see the Theoretical framework subsection). The turn motif does not force a peptide to adopt an intramolecular β-sheet conformation, but allows it to do so. If the peptide shows an intramolecular β-sheet conformation, the turn will most likely involve the turn motif YNGK. Both peptides showed 50–60 % β-sheet and 15–20 % β-turn according to CD. High levels of β-sheet are usually underestimated in calculations based on CD results [24]. Therefore, our results suggest that most of the residues are involved in the β-sheet. We conclude that the sheet is formed intramolecularly since it appeared at the first time point studied (1 min), and there was no concentration dependence on β-sheet content. Both peptides formed amyloid fibrils with the morphology of those formed by the decapeptide or Aβ. It could be argued that the intramolecular β-sheet may be lost during polymerization, and that the peptides polymerize in an 'open conformation' to form fibrils composed of parallel β-sheets. Cross-linking the peptides via terminal cysteines excluded this possibility. Cross-linking of the peptides did not give any significant changes in CD spectrum or fibril morphology. Thus both 'Dimer 1' and 'Dimer 2' are possible alignments and, moreover, peptides constrained to these alignments form fibrils.

Due to the nature of side-chain interactions in β-sheets, 28SS is forced to aggregate as in 'amyloid fibril model 1' (see the Theoretical framework subsection and Figure 3). The same considerations applied to 26SS give two possible aggregation patterns as in 'amyloid fibril model 2' or 'amyloid fibril model 3' (see the Theoretical framework subsection). Model 2 has a higher probability according to side-chain interactions, whereas model 3 will dominate if the contributions from van der Waals interactions and hydrogen bonds are more important (the values of these parameters are not clear, see the Theoretical framework subsection). A mixture of models 2 and 3 is also possible.

It is of interest to note that large amounts of fibrils were formed even at low concentrations of peptide. Thus the formation of a β-sheet containing the decapeptide, as would be in the case of dimer formation, could be the limiting step in fibril formation. The formation of an intramolecular β-sheet including an YNGK turn motif is not sufficient for fibril formation, as demonstrated by the 24SS and $28SS^{Val\text{-}Asp}$ peptides. Deletion of the glutamine residue in $A\beta^{14-23}$ gives a peptide incapable of forming fibrils, and the corresponding deletion of both glutamine residues in 26SS inhibited fibril formation. $28SS^{Val\text{-}Asp}$ formed a β-sheet (the probability of non-bonded Asp–Phe pairs which occur in the intramolecular β-sheet is 1.3), but did not form fibrils. This is explained by our model, where the intermolecular hydrogen-bonded Val–Phe pairs in 28SS ($P = 1.4$) are replaced by Asp–Phe pairs (zero probability with 99.5 % confidence).

We conclude from these studies that it is possible to construct fibrils of morphology identical to those generated by full-length Aβ from subunits constrained to have an antiparallel motif. This provides a 'proof of principle' for the antiparallel motif, and shows that it is possible to construct fibrils in which, by construction, at least 50 % of the alignments are antiparallel. Moreover, the fact that both 26SS and 28SS aggregated into fibrils demonstrates that at least two molecular structures, according to amyloid fibril models 1, 2 or 3, or a mixture of these are possible. The antiparallel alignment is in line with IR and X-ray diffraction results [12,13,18] and solid-state NMR studies on short Aβ fragments [29]. However, other solid-state NMR studies

on longer Aβ fragments indicate a parallel alignment [14,15,30], and it is possible that a subpopulation of peptides could adopt a parallel conformation or that fibril morphology depends strongly on preparation conditions. Another alternative is that the alignment is length-dependent, i.e. shorter sequences from a given peptide could have a stronger tendency to form antiparallel β-sheets [29].

The peptides 26SS and 28SS constrained to align according to model 1 or 2 have a strong tendency to form intramolecular β-sheets, corresponding to the Aβ-dimers in our model. These peptides rapidly form fibrils at low concentrations (1 μM, and possibly also at lower concentrations) compared with the decapeptide or Aβ (approx. 100 μM), indicating that the formation of an exposed β-sheet could be a rate-limiting step in polymerization. Interestingly, low amounts of stable Aβ-dimers form intracellularly [31] and can be found in cell cultures [31–33], in human cerebrospinal fluid [31] and in human brain [34]. The intracellular formation of Aβ-dimers could thus be the initial step in amyloidogenesis, offering an explanation as to why fibrils are formed despite the apparent low concentration of Aβ in the central nervous system.

It is interesting to note that substitution of only one residue in the decapeptide (two in the corresponding constrained peptides) blocks the formation of fibrils. It is possible that small organic compounds could induce similar small changes at the surface of the dimer. Another possibility to inhibit fibril formation is to block the formation of dimers. In both cases, the peptides used in this study should be useful in screens for such compounds. Preliminary experiments from this laboratory indicate that an energy-minimized model of the dimer is useful for computer analysis or simulation screening of compound libraries.

Finally, we suggest that the current approach using constrained structural subunits could be used to investigate the nature of interactions between sequences believed to be of importance for other amyloidogenic peptides and proteins.

This work was supported by the Swedish Research Council and Swedish Heart Lung Foundation (to J.T.), by Emma and Erik Granes Memorial Foundation (to L.O.T.) and by a grant from the Picower Foundation (to D.J.E.C.).

REFERENCES

1 Hardy, J. (1997) The Alzheimer family of diseases: many etiologies, one pathogenesis? [comment]. Proc. Natl. Acad. Sci. U.S.A. **94**, 2095–2097
2 Selkoe, D. J. (1999) Translating cell biology into therapeutic advances in Alzheimer's disease. Nature (London) **399**, A23–A31
3 Lorenzo, A. and Yankner, B. A. (1994) β-amyloid neurotoxicity requires fibril formation and is inhibited by Congo Red. Proc. Natl. Acad. Sci. U.S.A. **91**, 12243–12247
4 Iversen, L. L., Mortishire-Smith, R. J., Pollack, S. J. and Shearman, M. S. (1995) The toxicity *in vitro* of β-amyloid protein. Biochem. J. **311**, 1–16
5 Lambert, M. P., Barlow, A. K., Chromy, B. A., Edwards, C., Freed, R., Liosatos, M., Morgan, T. E., Rozovsky, I., Trommer, B., Viola, K. L. et al. (1998) Diffusible, nonfibrillar ligands derived from Aβ1–42 are potent central nervous system neurotoxins. Proc. Natl. Acad. Sci. U.S.A. **95**, 6448–6453
6 Hartley, D. M., Walsh, D. M., Ye, C. P., Diehl, T., Vasquez, S., Vassilev, P. M., Teplow, D. B. and Selkoe, D. J. (1999) Protofibrillar intermediates of amyloid β-protein induce acute electrophysiological changes and progressive neurotoxicity in cortical neurons. J. Neurosci. **19**, 8876–8884
7 Talafous, J., Marcinowski, K. J., Klopman, G. and Zagorski, M. G. (1994) Solution structure of residues 1–28 of the amyloid β-peptide. Biochemistry **33**, 7788–7796
8 Sticht, H., Bayer, P., Willbold, D., Dames, S., Hilbich, C., Beyreuther, K., Frank, R. W. and Rosch, P. (1995) Structure of amyloid A4-(1–40)-peptide of Alzheimer's disease. Eur. J. Biochem. **233**, 293–298
9 Shao, H., Jao, S., Ma, K. and Zagorski, M. G. (1999) Solution structures of micelle-bound amyloid β-(1–40) and β-(1–42) peptides of Alzheimer's disease. J. Mol. Biol. **285**, 755–773
10 Tjernberg, L. O., Pramanik, A., Bjorling, S., Thyberg, P., Thyberg, J., Nordstedt, C., Berndt, K. D., Terenius, L. and Rigler, R. (1999) Amyloid β-peptide polymerization studied using fluorescence correlation spectroscopy. Chem. Biol. **6**, 53–62
11 Inouye, H., Fraser, P. E. and Kirschner, D. A. (1993) Structure of β-crystallite assemblies formed by Alzheimer β-amyloid protein analogues: analysis by X-ray diffraction. Biophys. J. **64**, 502–519
12 Serpell, L. C. and Smith, J. M. (2000) Direct visualisation of the β-sheet structure of synthetic Alzheimer's amyloid. J. Mol. Biol. **299**, 225–231
13 Hilbich, C., Kisters-Woike, B., Reed, J., Masters, C. L. and Beyreuther, K. (1991) Aggregation and secondary structure of synthetic amyloid β A4 peptides of Alzheimer's disease. J. Mol. Biol. **218**, 149–163
14 Benzinger, T. L., Gregory, D. M., Burkoth, T. S., Miller-Auer, H., Lynn, D. G., Botto, R. E. and Meredith, S. C. (1998) Propagating structure of Alzheimer's β-amyloid(10–35) is parallel β-sheet with residues in exact register. Proc. Natl. Acad. Sci. U.S.A. **95**, 13407–13412
15 Benzinger, T. L., Gregory, D. M., Burkoth, T. S., Miller-Auer, H., Lynn, D. G., Botto, R. E. and Meredith, S. C. (2000) Two-dimensional structure of β-amyloid(10–35) fibrils. Biochemistry **39**, 3491–3499
16 Tjernberg, L. O., Naslund, J., Lindqvist, F., Johansson, J., Karlstrom, A. R., Thyberg, J., Terenius, L. and Nordstedt, C. (1996) Arrest of β-amyloid fibril formation by a pentapeptide ligand. J. Biol. Chem. **271**, 8545–8548
17 Tjernberg, L. O., Lilliehook, C., Callaway, D. J., Naslund, J., Hahne, S., Thyberg, J., Terenius, L. and Nordstedt, C. (1997) Controlling amyloid β-peptide fibril formation with protease-stable ligands. J. Biol. Chem. **272**, 12601–12605. Published erratum appears in J. Biol. Chem. (1997) **272**(28), 17894
18 Inouye, H. and Kirschner, D. A. (1996) Refined fibril structures: the hydrophobic core in Alzheimer's amyloid β-protein and prion as revealed by X-ray diffraction. Ciba Found. Symp. **199**, 22–35
19 Pike, C. J., Walencewicz-Wasserman, A. J., Kosmoski, J., Cribbs, D. H., Glabe, C. G. and Cotman, C. W. (1995) Structure-activity analyses of β-amyloid peptides: contributions of the β 25–35 region to aggregation and neurotoxicity. J. Neurochem. **64**, 253–265
20 Tjernberg, L. O., Callaway, D. J., Tjernberg, A., Hahne, S., Lilliehook, C., Terenius, L., Thyberg, J. and Nordstedt, C. (1999) A molecular model of Alzheimer amyloid β-peptide fibril formation. J. Biol. Chem. **274**, 12619–12625
21 Wouters, M. A. and Curmi, P. M. (1995) An analysis of side chain interactions and pair correlations within antiparallel β-sheets: the differences between backbone hydrogen-bonded and non-hydrogen-bonded residue pairs. Proteins **22**, 119–131
22 Yang, A. S. and Honig, B. (1995) Free energy determinants of secondary structure formation: II. Antiparallel β-sheets. J. Mol. Biol. **252**, 366–376
23 Ellman, G. L. (1959) Tissue sulfhydryl groups. Arch. Biochem. Biophys. **82**, 70–77
24 Greenfield, N. J. (1996) Methods to estimate the conformation of proteins and polypeptides from circular dichroism data. Anal. Biochem. **235**, 1–10
25 Hutchinson, E. G. and Thornton, J. M. (1994) A revised set of potentials for β-turn formation in proteins. Protein Sci. **3**, 2207–2216
26 Naslund, J., Schierhorn, A., Hellman, U., Lannfelt, L., Roses, A. D., Tjernberg, L. O., Silberring, J., Gandy, S. E., Winblad, B., Greengard, P. et al. (1994) Relative abundance of Alzheimer Aβ amyloid peptide variants in Alzheimer disease and normal aging. Proc. Natl. Acad. Sci. U.S.A. **91**, 8378–8382
27 Wang, R., Sweeney, D., Gandy, S. E. and Sisodia, S. S. (1996) The profile of soluble amyloid β protein in cultured cell media. Detection and quantification of amyloid β protein and variants by immunoprecipitation–mass spectrometry. J. Biol. Chem. **271**, 31894–31902
28 Jarrett, J. T., Berger, E. P. and Lansbury, Jr, P. T. (1993) The carboxy terminus of the β amyloid protein is critical for the seeding of amyloid formation: implications for the pathogenesis of Alzheimer's disease. Biochemistry **32**, 4693–4697
29 Balbach, J. J., Ishii, Y., Antzutkin, O. N., Leapman, R. D., Rizzo, N. W., Dyda, F., Reed, J. and Tycko, R. (2000) Amyloid fibril formation by Aβ 16–22, a seven-residue fragment of the Alzheimer's β-amyloid peptide, and structural characterization by solid state NMR. Biochemistry **39**, 13748–13759
30 Antzutkin, O. N., Balbach, J. J., Leapman, R. D., Rizzo, N. W., Reed, J. and Tycko, R. (2000) Multiple quantum solid-state NMR indicates a parallel, not antiparallel, organization of β-sheets in Alzheimer's β-amyloid fibrils. Proc. Natl. Acad. Sci. U.S.A. **97**, 13045–13050
31 Walsh, D. M., Tseng, B. P., Rydel, R. E., Podlisny, M. B. and Selkoe, D. J. (2000) The oligomerization of amyloid β-protein begins intracellularly in cells derived from human brain. Biochemistry **39**, 10831–10839
32 Podlisny, M. B., Ostaszewski, B. L., Squazzo, S. L., Koo, E. H., Rydell, R. E., Teplow, D. B. and Selkoe, D. J. (1995) Aggregation of secreted amyloid β-protein into sodium dodecyl sulfate-stable oligomers in cell culture. J. Biol. Chem. **270**, 9564–9570

33 Podlisny, M. B., Walsh, D. M., Amarante, P., Ostaszewski, B. L., Stimson, E. R., Maggio, J. E., Teplow, D. B. and Selkoe, D. J. (1998) Oligomerization of endogenous and synthetic amyloid β-protein at nanomolar levels in cell culture and stabilization of monomer by Congo Red. Biochemistry **37**, 3602–3611

34 Roher, A. E., Chaney, M. O., Kuo, Y. M., Webster, S. D., Stine, W. B., Haverkamp, L. J., Woods, A. S., Cotter, R. J., Tuohy, J. M., Krafft, G. A. et al. (1996) Morphology and toxicity of Aβ-(1–42) dimer derived from neuritic and vascular amyloid deposits of Alzheimer's disease. J. Biol. Chem. **271**, 20631–20635

Received 6 February 2002/15 May 2002; accepted 22 May 2002
Published as BJ Immediate Publication 22 May 2002, DOI 10.1042/BJ20020229